Synthesis, spectral studies and antimicrobial screening of metal complexes of Schiff base derived from substituted salicylaldehyde and 2-amino-6-chloro benzothiazole

Dipti D. Gharat[1], Kirti P. Mhatre[2], Ramesh S. Yamgar[3], Shashikant D. Ajagekar[1*]

[1]Department of Chemistry, Thakur College of Science and Commerce, Kandivali (East), Mumbai, Maharashtra, India-400 101.
[2]Department of Chemistry, VWTCT'S Bhaskar Waman Thakur College of Science, Virar (West), Maharashtra, India-401303.
[3]Department of Chemistry, CS's S.S. & L.S. Patkar College of Arts & Science, and V. P. Varde College of Commerce & Economics, Goregaon (West), Mumbai, India-400062.

***Corresponding Author:** Shashikant D. Ajagekar
drsdajagekartcsc@gmail.com

Abstract
In the present work Schiff base ligand of benzaldehyde derivative and benzothiazole derivatives was prepared by condensation of 2-amino-6-chloro benzothiazoles and 2, 4-dihydroxybenzaldehyde in a 1:1 molar ratio. It was further treated with bivalent metal salts, resulting in a series of transition metal complexes of the type $[M(CBTIHB)_2]$ [M = Fe, Cu, Co, Ni, Pd, Zn, Hg, and Cd]. The prepared Schiff base HCBTIHB ligand and its bivalent metal complexes were studied using different spectroscopic techniques (^{1}H NMR, FT-IR, UV) and physicochemical methods. By using the disc diffusion method, two Gram-positive bacterial strains (*B. subtilis* and *S. aureus*) and two Gram-negative bacterial strains (*E. coli* and *P. aeruginosa*), as well as two fungal strains (*C. albicans* and *A. cerevisiae*) were used to test all of the synthesized compounds for antibacterial and antifungal activity in vitro. The spectrum data showed the complexes were hexacoordinated with tridentate ligands, coordinated through oxygen, sulphur, and nitrogen. The XRD data has been analyzed using the advanced Professional program. Particle size, crystal system, lattice parameter, and lattice type had all been approximated from the experimental data. The particle size was measured on the nanoscale scale. All of the complexes were found to be crystalline after being subjected to XRD examination. The results of antimicrobial activity showed that the synthesized complexes were more effective in Gram-positive bacterial strains than in Gram-negative bacterial strains. The in vitro cytotoxicity effects of the ligand and its metal complexes against *Artemia salina* were also investigated using the brine shrimp bioassay. The results demonstrated that biological activities of the ligand were enhanced during complexation.

Keywords: Disc diffusion method, potent antibacterial activities, bivalent metal complexes.

Introduction:
The metal-based drug development is undergoing explosive expansion and the need for pharmaceutical treatments are the primary motivating factor. Transition metal complexes shown promising results, which has prompted more targeted studies in this field [1-3]. Transition metal complexes are unique in their synthesis and structure, where the ligands that bond to the fundamental metal allow for a wide range of potential applications [4, 5]. Due to their interesting structural possibilities, transition metal complexes exhibited the most diverse applications spanning industrial, catalysis, and therapeutics [6-11]. Insecticidal, antibacterial, antifungal, anti-inflammatory and anticancer effects are intriguing chemotherapeutic uses for Schiff bases [12–17].

Due to their potent biological activity transition metal complexes of Schiff bases have developed as promising platforms for developing new therapeutics. Schiff bases and metal complexes exhibit various potential applications [18]. Benzothiazoles are flexible fused heterocyclic scaffolds with extensive pharmaceutical applications. They are the subject of intensive research due to their structural diversity, adaptability, high thermal stability and medicinal efficacy [19, 20]. They have many uses in drug development and are mostly found in bio-inorganic and medicinal chemistry. The benzothiazole nucleus is used in the synthesis of numerous medicines. Because of their wide range of biological activity, including anticancer, antitubercular, anti-HIV, cardiovascular, local anesthetic, anti-inflammatory, anticonvulsant, and anti-diabetic effects, benzothiazoles have attracted great interest. They were used as the central nucleus in a wide variety of drugs. The chemists have been inspired by the therapeutic potential of benzothiazoles to synthesize a wide variety of new chemotherapeutic drugs [21, 22]. Due to their ease of synthesis, substituted 2-arylbenzothiazoles have recently gained attention as a significant pharmacophore with various therapeutic and analytical features [23].

Because of these, synthesized and analyzed the spectra of transition metal complexes of Schiff bases of 2-amino-6-substituted-benzothiazole derivatives and tested their antibacterial properties and antifungal activities.

Experimental:

Materials and methods:

The chemicals used were purchased from BLD Pharma. All solvents were received from Loba Chemie and used after drying as per usual protocols; all were of analytical research-grade quality. Brucker FT-IR spectra were obtained from 4000-400 cm^{-1} using a spectrometer. The Bruker Advance II 400 MHz NMR spectrometer was used to record the NMR spectra of the substances. TMS was used as the internal standard in DMSO-d_6 for ^1H NMR spectroscopy. After decomposition with intense HNO_3, metal (II) was measured using a volumetric method [24]. An electrical heating coil device was used to record the melting points. Electronic absorption spectra were recorded on a JASCO V650 spectrophotometer at room temperature. The spectrophotometer BRUKER D8 VENTURE was used to record powder XRD patterns of the compounds.

Synthesis of HCBTIHB ligand:

2, 4-Dihydroxybenzaldehyde (10 mmol), 2-amino-6-chlorobenzothiazoles (10 mmol) and 2-3 drops of hydrochloric acid were dissolved in an ethanolic solution and refluxed for 2 hours at room temperature. Filtered the yellow solid product, washed and recrystallized with ethanol yielding a pure solid. Thin-layer chromatography (TLC) was routinely used to test the purity of the compound. Yield: 68.79%; yellow solid; melting point: 165 °C; (Mol. Wt. 304.75); Anal Calcd. for $C_{14}H_9N_2O_2SCl$ (%): C, 55.18; H, 2.98; N, 9.19; O, 10.50; S, 10.50; Cl, 11.63. Observed: C, 55.03; H, 2.97; N, 9.16; O, 10.24; S, 10.33; Cl, 11.60. IR (KBr pellets, cm^{-1}): 3351 (O-H), 3260 (O-H), 2971 (-CH=), 1653 (>C=N), 1590/1489 (>C=C<), 1452 (Ar C-N), 1347 (C-O), 1294 (C-S). ^1H NMR (DMSO-d_6, ppm, 400 MHz): 12.98 (1H, s, O–H), 12.56 (1H, s, O-H), 7.93 (1H, s, HC=N), 7.00-7.67 (7H, m, Ar–H). UV spectra (λ_{nm}) 383, 298.

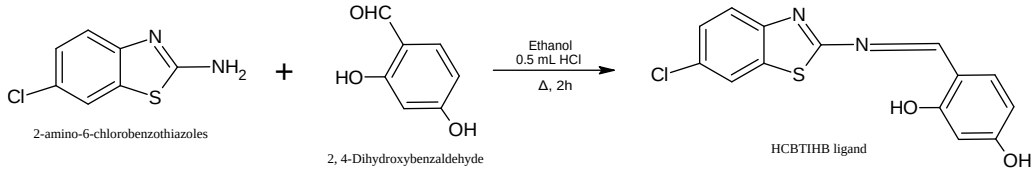

Scheme 1: Preparation of HCBTIHB ligand

Synthesis of complexes:

Synthesis of transition metal complexes (M = Fe, Cu, Co, Ni, Pd, Zn, Hg, and Cd) was carried out by reacting HCBTIHB with the respective metal chlorides. A dilute alkali was used to adjust the pH of a mixture at 7 containing 10 mmol of HCBTIHB ligand and 5 mmol of metal chlorides. The reaction mixture was refluxed for 2 hours. The separation of solid complexes was followed by filtration, washing with ethanol and collection of solid .Chloroform and diethyl ether (1:1, v/v) were used to recrystallize the substance after it was collected.

Bis(4-{[(6-chloro-1,3-benzothiazol-2-yl)imino]methyl}benzene-1,3-diol)ferrous(II):

Yield: 78.53%; blue solid; melting point: 193 °C; (Mol. Wt. 663.34); Anal. Calcd for $C_{28}H_{16}N_4O_4S_2Cl_2Fe$ (%): C, 50.65; H, 2.41; N, 8.44; O, 9.65; S, 9.65; Cl, 10.70; Fe, 8.42. Observed: C, 50.47; H, 2.18; N, 8.39; O, 9.29; S, 9.39; Cl, 10.63; Fe, 8.32. IR (KBr pellets, cm^{-1}): 3224 (O-H), 3033 (-CH=), 1633 (>C=N), 1586/1450 (>C=C<), 1412 (Ar C-N), 1302 (C-O), 1232 (C-S), 607 (N→M), 536 (S→M), 507(O-M). UV spectra (λ_{nm}) 601, 483.

Bis(4-{[(6-chloro-1,3-benzothiazol-2-yl)imino]methyl}benzene-1,3-diol)cobalt(II):

Yield: 84.60%; brown solid; melting point: 199 °C; (Mol. Wt. 668.34); Anal. Calcd for $C_{28}H_{16}N_4O_4S_2Cl_2Co$ (%): C, 50.65; H, 2.41; N, 8.44; O, 9.65; S, 9.65; Cl, 10.70; Co, 8.89. Observed: C, 50.43; H, 2.16; N, 8.33; O, 9.38; S, 9.42; Cl, 10.61; Co, 8.80. IR (KBr pellets, cm^{-1}): 3268 (O-H), 3031 (-CH=), 1585 (>C=N), 1535/1480 (>C=C<), 1412 (Ar C-N), 1303 (C-O), 1227 (C-S), 560 (N→M), 537 (S→M), 511(O-M). UV spectra (λ_{nm}) 892, 511, 425, 399, 312.

Bis(4-{[(6-chloro-1,3-benzothiazol-2-yl)imino]methyl}benzene-1,3-diol)nickel(II):

Yield: 69.88%; brown solid; melting point: 199 °C; (Mol. Wt. 668.19); Anal. Calcd for $C_{28}H_{16}N_4O_4S_2Cl_2Ni$ (%): C, 50.28; H, 2.39; N, 8.38; O, 9.58; S, 9.58; Cl, 10.60; Ni, 8.78. Observed: C, 50.00; H, 2.38; N, 8.36; O, 9.37; S, 9.49; Cl, 10.55; Ni, 8.69. IR (KBr pellets, cm^{-1}): 3270 (O-H), 3033 (-CH=), 1631 (>C=N), 1585/1450 (>C=C<), 1411 (Ar C-N), 1303 (C-O), 1208 (C-S), 637 (N→M), 607 (S→M), 511(O-M). UV spectra (λ_{nm}) 985, 630, 451.

Bis(4-{[(6-chloro-1,3-benzothiazol-2-yl)imino]methyl}benzene-1,3-diol)palldium(II):

Yield: 82.98%; orange solid; melting point: 205 °C; (Mol. Wt. 715.50); Anal. Calcd for $C_{28}H_{16}N_4O_4S_2Cl_2Pd$ (%): C, 46.96; H, 2.24; N, 7.83; O, 8.94; S, 8.94; Cl, 9.92; Pd, 14.81. Observed: C, 46.88; H, 2.19; N, 7.77; O, 8.90; S, 8.92; Cl, 9.91; Ni, 14.73. IR (KBr pellets, cm^{-1}): 3268 (O-H), 3023 (-CH=), 1632 (>C=N), 1533/1449 (>C=C<), 1409 (Ar C-N), 1301 (C-O), 1271 (C-S), 540 (N→M), 511(O-M). UV spectra (λ_{nm}) 351, 312, 280.

Bis(4-{[(6-chloro-1,3-benzothiazol-2-yl)imino]methyl}benzene-1,3-diol)copper(II):
Yield: 76.79%; brown solid; melting point: 199 °C; (Mol. Wt. 673.05); Anal. Calcd for $C_{28}H_{16}N_4O_4S_2Cl_2Cu$ (%): C, 49.92; H, 2.38; N, 8.32; O, 9.51; S, 9.51; Cl, 10.50; Cu, 9.44. Observed: C, 49.89; H, 2.35; N, 8.30; O, 9.44; S, 9.47; Cl, 10.43; Cu, 9.89. IR (KBr pellets, cm^{-1}): 3270 (O-H), 3029 (-CH=), 1633 (>C=N), 1533/1452 (>C=C<), 1409 (Ar C-N), 1302 (C-O), 1269 (C-S), 604 (N→M), 538 (S→M), 507(O-M). UV spectra (λ_{nm}) 500, 416, 307.

Bis(4-{[(6-chloro-1,3-benzothiazol-2-yl)imino]methyl}benzene-1,3-diol)zinc(II):
Yield: 69.76%; yellow solid; melting point: 195 °C; (Mol. Wt. 674.89); Anal. Calcd for $C_{28}H_{16}N_4O_4S_2Cl_2Zn$ (%): C, 49.79; H, 2.37; N, 8.30; O, 9.48; S, 9.48; Cl, 10.50; Zn, 9.69. Observed: C, 49.66; H, 2.35; N, 8.22; O, 9.42; S, 9.40; Cl, 10.37; Zn, 9.55. IR (KBr pellets, cm^{-1}): 3294 (O-H), 3066 (-CH=), 1601 (>C=N), 1568/1433 (>C=C<), 1338 (C-O), 1274 (C-S), 611 (N→M), 541(O-M). UV spectra (λ_{nm}) 348, 271.

Bis(4-{[(6-chloro-1,3-benzothiazol-2-yl)imino]methyl}benzene-1,3-diol)cadmium(II):
Yield: 79.86%; yellow solid; melting point: 203 °C; (Mol. Wt. 721.91); Anal. Calcd for $C_{28}H_{16}N_4O_4S_2Cl_2Cd$ (%): C, 46.54; H, 2.22; N, 7.76; O, 8.87; S, 8.87; Cl, 7.74; Cd, 15.57. Observed: C, 46.54; H, 2.19; N, 7.70; O, 8.88; S, 8.86; Cl, 7.73; Cd, 15.51. IR (KBr pellets, cm^{-1}): 3228 (O-H), 2921 (-CH=), 1578 (>C=N), 1535 (>C=C<), 1432 (Ar C-N), 1309 (C-O), 1215 (C-S), 571 (N→M), 532(O-M). UV spectra (λ_{nm}) 362, 348, 278.

Bis(4-{[(6-chloro-1,3-benzothiazol-2-yl)imino]methyl}benzene-1,3-diol)mercury(II):
Yield: 67.17%; red solid; melting point: 207 °C; (Mol. Wt. 869.50); Anal. Calcd for $C_{28}H_{16}N_4O_4S_2Cl_2Hg$ (%): C, 41.51; H, 1.98; N, 6.92; O, 9.91; S, 9.91; Cl, 4.39; Hg, 24.78. Observed: C, 41.41; H, 1.97; N, 6.89; O, 9.86; S, 7.85; Cl, 4.38; Hg, 24.66. IR (KBr pellets, cm^{-1}): 3266 (O-H), 2926 (-CH=), 1585 (>C=N), 1411 (Ar C-N), 1266 (C-S), 531 (N→M), 511(O-M). UV spectra (λ_{nm}) 322, 277.

Bis(4-{[(6-chloro-1,3-benzothiazol-2-yl)imino]methyl}benzene-1,3-diol)manganese(II):
Yield: 73.44%; brown solid; melting point: 210 °C; (Mol. Wt. 662.44); Anal. Calcd for $C_{28}H_{16}N_4O_4S_2Cl_2Mn$ (%): C, 50.72; H, 2.42; N, 8.45; O, 9.66; S, 9.66; Cl, 10.70; Mn, 8.29. Observed: C, 50.29; H, 2.34; N, 8.43; O, 9.39; S, 9.59; Cl, 10.59; Mn, 8.22. IR (KBr pellets, cm^{-1}): 3225 (O-H), 3032 (-CH=), 1632 (>C=N), 1586/1480 (>C=C<), 1412 (Ar C-N), 1302 (C-O), 1266 (C-S), 605 (N→M), 541 (S→M), 510(O-M). UV spectra (λ_{nm}) 535.

Antimicrobial Studies:
The minimum inhibitory concentration (MIC) of the compounds against several bacterial and fungal strains was determined by serial dilution testing in vitro [25]. Test tubes containing 1 mL of nutrient medium were autoclaved for 30 minutes at 100 °C and fungal and bacterial strains were grown on Sabouraud dextrose agar and nutrient broth respectively. Compounds were produced as 100 µg/mL DMSO stock solutions, which were then diluted to yield final concentrations of 50, 25, 12.5, 6.25, 3.12, and 1.56 µg/mL. Each test tube was inoculated with 100 µg/mL of a freshly cultivated strain in normal saline and incubated at 25 °C for 7 days for fungal strains and incubated at 37 °C for 24 hrs for bacterial strains. Triplicate determinations of each sample's MIC were determined.

Cytotoxicity:
The newly synthesized HCBTIHB ligand and its Cu(II), Fe(II), Co(II), Pd(II), Ni(II), Mn(II), Cd(II), Hg(II) and Zn(II) complexes were tested *in vitro* for their cytotoxic effects using the brine shrimp lethality bioassay according to the technique. This assay correlates well with cytotoxic activity and is quick and cheap to conduct. Eggs of the brine shrimp (*Artemia salina*) species were incubated in artificial seawater made from a commercial salt mixture and double-distilled water in a shallow rectangular plastic dish. A perforated tool was used to divide the plastic dish into two halves. The main container contained around 50 mg of eggs, while the smaller compartment, which was open to normal light, contained about 10 mg. The *nauplii* were pipetted from the illuminated side after two days. To make a sample of 20 mg the test compounds were dissolved in 2 mL of dimethyl sulfoxide (DMSO). Nine vials were filled from the stock solution at concentrations of 100, 50, and 25 µg/mL (three of each dilution were used for each test sample and the LD_{50} is the average of three values) and one vial was preserved as a control containing 2 mL of DMSO only, the solvent was left to evaporate. When the shrimp larvae were ready after two days, 1 mL of seawater and 10 shrimps were put into each vial, with the volume increased with seawater to 10 mL each vial (30 shrimps/dilution). The count of those still alive was taken after 24 hours. The LD_{50} values were calculated using a Finney computer program.

Results and Discussion:
The synthesis of 4-{[(6-chloro-1,3-benzothiazol-2-yl)imino]methyl}benzene-1,3-diol was prepared through the reaction between 2, 4-hydroxybenzaldehyde and 2-amino-6-chloro-benzothiazole. Subsequently, the resulting compound was subjected to further reactions with appropriate metal chlorides and prepared metal complexes. The compounds of evaluation were identified as colored substances that exhibited solubility in DMSO, acetonitrile and nitrobenzene. TLC assessed the purity of the compounds. The synthetic procedure for the Schiff base ligand and its divalent complexes is depicted in **Scheme 1.** The conductance measurements were obtained for solutions of the metal complexes in nitrobenzene

with a concentration of 10^{-3} M. All complexes exhibit non-conductivity, which suggests their neutrality and the replacement of phenolic and imine protons by divalent cations.

Magnetic moments and electronic spectral data of the ligand and its metal complexes:
The UV-VIS spectrum was obtained for the ethanolic solution of the HCBTIHB ligand. It exhibited absorption bands at 298nm, which were attributed to $\pi\rightarrow\pi^*$ transitions occurring inside the aromatic ring. The observed band at a wavelength of 383nm can be attributed to the $n\rightarrow\pi^*$ transition of the C=N functional group.

In the UV range of metal complexes spectra, it is commonly noted that the absorption bands resulting from $\pi\rightarrow\pi^*$ and $n\rightarrow\pi^*$ transitions, which are initially detected at wavelengths greater than 383 nm in the spectrum of the unbound ligand, undergo a redshift as a consequence of ligand coordination with metal ions.
The electronic spectra of the Fe(II) complex exhibited a broad band at a wavelength of 601 nm. The observed disappearance of the previous band can perhaps be the spin-forbidden transition $^5T_{2g}\rightarrow{}^5E_g$. This transition exhibited increased intensity due to the vibrionic mechanism occurring within the octahedral field surrounding the ferric ion. The charge transfer transition is allocated to the second absorption band, which exhibits a high intensity at 483nm. The magnetic moment of the complex is measured to be 5.16 B.M. The observed value is significantly lower than the calculated magnetic moment value for binuclear iron complexes [26].

The Co(II) complex has a magnetic moment of 4.59 B.M., suggesting the presence of a Co(II) ion in an octahedral coordination geometry. The complex exhibited two *d-d* transitions in its electronic spectrum, specifically at wavelengths of 892nm and 511nm. These transitions attributed to the $^4T_{1g}(F) \rightarrow {}^4A_{2g}(F)$ and $^4T_{1g}(F) \rightarrow {}^4A_{2g}(P)$ transitions, respectively [27]. This observation suggests the presence of an octahedral coordination geometry surrounding Co(II) ions.

The mononuclear Ni(II) complex exhibited a broad absorption spectrum in the visible range. Specifically, absorption bands were observed at 985nm and 630nm wavelengths. These bands can be attributed to the $^3A_{2g}$ (F) $\rightarrow {}^3T_{2g}(F)\ \upsilon_1$ and $^3A_{2g}$ (F) $\rightarrow {}^3T_{1g}(F)\ \upsilon_2$ transitions, respectively. However, it should be noted that the absorption resulting from the $^3A_{2g}(F)\rightarrow{}^3T_{1g}(P)$ transition overlaps with the absorption bands of the ligand. This suggests that the Ni(II) ion is coordinated to $N_2O_2S_2$ sites in an octahedral geometry [28, 29].
The Ni(II) ion achieved a coordination number of six. The third transition resulting from the $^3A_{2g}(F)\rightarrow{}^3T_{1g}(P)$ process would exceed the measurement range of the employed spectrophotometer. The complex has a magnetic moment of 3.00 B.M. indicating the presence of a Ni(II) ion in an octahedral geometry.

The absorption spectrum of the mononuclear Cu(II) complex exhibited a distinct absorption band at a wavelength of 500nm. This absorption band can be ascribed to the $^2A_{1g}\rightarrow{}^2B_{1g}$ this transition associated with the Cu(II) ion in a square-planar geometry [30].

The confirmed square-planar geometry of the Cu(II) ion in the complex is supported by the measured magnetic moment values, which were found to be 1.91 B.M. The square-planar geometry is attained by coordinating two molecules of the ligand, each functioning as a monobasic bidentate ligand, to the Cu(II) ion [31].

An absorption band at a wavelength of 535nm was seen in the spectra of the Mn (II) complex. This band has characteristics of both Laporte and spin-forbidden properties. The presence of weak bands might occasionally be attributed to the rapid distortion of octahedral structures surrounding the metal cations [32].

IR spectra:
The Fourier-transform infrared (FT-IR) spectra of the HCBTIHB ligand and its complexes were obtained by employing KBr pellets as the sample matrix. The assignment of coordination sites of the ligand occurred through a comparative analysis of the infrared spectra of the corresponding Schiff bases and their respective divalent complexes. The confirmation of the hydroxyl group in the HCBTIHB ligand was achieved by observing a wide absorption band at 3351 cm^{-1}, which was attributed to the presence of the hydroxyl group (OH) of the C2 phenyl ring. The disappearance of the wide absorption band associated with the hydroxyl group can be attributed to the deprotonation of the complexes phenolic (C2) group. This suggests that the oxygen atom is bonded to the central metal atom. A broad absorption band at 3224-3294 cm^{-1} due to υ(OH) showed that the HCBTIHB ligand and its metal complexes had a hydroxyl group. The aromatic υ(C-S) in the HCBTIHB ligand is caused by the middle-intensity absorption band with a stretching frequency of 1247 cm^{-1}. In complexes, the sulfur group's absorption band moved by 8-41 cm^{-1} towards lower frequencies with a middle level of intensity. This suggested that the sulfur atom is linked to the metal atom. The absorption band characterized by a moderate intensity and a stretching frequency of 1653 cm^{-1}, was assigned to the presence of the (C=N) bond in the azomethine group of the ligand. The absorption band corresponding to the azomethine group exhibited a downward shift of 20-75 cm^{-1} in complexes indicating potential coordination between the nitrogen and metal ions. The strength of this shift was moderate. The detected absorption bands within the ranges of 560-631, 531-541 and 510-511 cm^{-1} were assigned

to the vibrations of υ(S→M), υ(N→M), and υ(O-M) accordingly. These observations suggested the coordination of sulfur, oxygen, and nitrogen to the central metal atom [33, 34].

^{1}H NMR spectra:
The HCBTIHB ligand and its complexes were dissolved in DMSO-d_6 to obtain ^{1}H NMR spectra. Chemical shifts, integration values and coupling constants were used to deduce the ^{1}H NMR spectra of the substances. The signal at δ12.98 and δ12.56 ppm was determined which originated from the phenolic C2 and C4 protons respectively, in the HCBTIHB ligand. Confirming the condensation of 2-amino-6-chloro-benzothiazole with 2, 4-dihydroxybenzaldehyde. A signal at δ7.932 ppm indicated the existence of azomethine proton in the HCBTIHB ligand. The presence of powerful electron-withdrawing groups in the compound resulted in signals at δ7.00-7.67 ppm, which were attributed to the aryl protons of the HCBTIHB ligand. Coupling constants, integration and chemical shift values were used to compare the ^{1}H NMR spectra of the complexes of the HCBTIHB ligand. The disappearance of phenolic C2 proton signal in all transition metal complexes indicates phenolic C2 proton deprotonation and metal ion coordination. Because of the deshielding effect caused by the coordination of the nitrogen atom of the imino moiety to the central metal atom. There was a little shift in the proton signals of the azomethine group. As reported [35–37]. Aryl and alkyl group signals were observed as reported.

X-Ray Diffraction Study:
Intense peaks in the X-ray diffractograms of the metal complexes under study indicated high crystallinity. Computational studies for cobalt and nickel complexes of HCBTIHB ligand yielded lattice parameter values of $a \neq b \neq c$ and $\alpha = \beta = \gamma$, indicating an Orthorhombic Crystal Structure of a P-type lattice. The tetragonal crystal structure of the P-type lattice is suggested by lattice parameter values of $a = b \neq c$ and $\alpha = \beta = \gamma$ for a copper complex of HCBTIHB ligand. The ferrous complex has lattice parameters $a = b \neq c$ and $\alpha = \gamma \neq \beta$, indicating a monoclinic crystal structure of a P-type lattice. The values of the lattice parameters $a \neq b \neq c$ and $\alpha = \gamma \neq \beta$ for the manganese complex suggest a hexagonal crystal structure with a P-type lattice.

Antibacterial and antifungal activity:
The antibacterial activity of all synthesized compounds was assessed in vitro against Gram-negative bacteria, including *Escherichia coli* and *Pseudomonas aeruginosa*, as well as Gram-positive bacteria, including *Bacillus subtilis* and *Staphylococcus aureus*. The activity against fungi, such as *Candida albicans* and *Saccharomyces cerevisiae*, was also tested. *Streptomycin* and *fluconazole* were employed as conventional pharmaceutical agents to exhibit antibacterial and antifungal properties, respectively. The disc diffusion method was employed to assess the antibacterial activity. **Table 1** displays antimicrobial activity findings. The minimum inhibitory concentration (MIC) was measured in μM/mL. The antibacterial and antifungal activity findings demonstrated that $Hg(CBTIHB)_2$ had the highest efficacy against all kinds of microorganisms. The ligands exhibited the lowest activity against microorganisms. The antibacterial activity followed the order of Hg > Cu > Fe > Co > Ni > Mn > Pd > Cd > Zn. Based on the reported data a significant increase was observed in the activity of complexes compared to the ligand. The observed enhancement in antibacterial activity of the synthesized complexes is attributed to the process of chelation, which exhibits greater potency and efficacy as an antimicrobial agent [38-41].

Table 1: Antibacterial and antifungal activity data of HCBTIHB and its metal complexes

Compound	***B. subtilis***	***P. aeruginosa***	***S. aureus***	***E. coli***	***C albicans***	***S. cerevisiae***
HCBTIHB	7.05	6.12	7.25	7.95	8.85	8.44
$Fe(CBTIHB)_2$	9.22	18.25	19.22	18.25	18.19	8.14
$Co(CBTIHB)_2$	11.22	19.04	12.22	19.04	18.22	8.03
$Ni(CBTIHB)_2$	9.23	19.14	14.29	19.14	13.45	10.48
$Pd(CBTIHB)_2$	12.05	11.44	12.65	11.44	9.77	-
$Cu(CBTIHB)_2$	17.22	17.12	17.20	15.68	17.21	7.02
$Zn(CBTIHB)_2$	9.48	7.25	14.45	9.48	19.22	9.68
$Cd(CBTIHB)_2$	13.45	9.11	15.18	9.17	12.74	-
$Hg(CBTIHB)_2$	18.14	17.04	15.19	17.25	10.29	10.47
$Mn(CBTIHB)_2$	10.44	9.55	10.37	19.47	13.35	11.22
Streptomycin	16.12	15.88	15.19	15.88	NA	NA
fluconazole	NA	NA	NA	NA	19.23	18.19

Cytotoxicity:
The brine shrimp bioassay evaluated the cytotoxicity of all the synthesized compounds, by following the procedure established by Meyer *et al*. [42]. It is apparent, based on the data, that the synthesized metal complexes exhibited more cytotoxic activity compared to the free uncoordinated ligand.

Conclusions:

The evaluations of data provided evidence to support the proposed structures of the metal complexes. The metal cation complexes of Fe(II), Ni(II), Co(II) and Mn(II) exhibited an octahedral geometry, whereas the Cu(II) and Pd(II) complexes displayed a square planar geometry and Hg, Cd, Zn, complexes were tetrahedral in nature. According to the data shown in **Table 1**, it can be observed that all substances had significant efficacy in inhibiting and eradicating microorganisms when used at concentrations of 100%. It has been observed that complexes of Hg(II), Fe(II), Co(II) and Ni(II) had shown more potent antibacterial activities as compared to standard *Streptomycin*. Based on spectral studies, structures of metal complexes are assigned as follows;

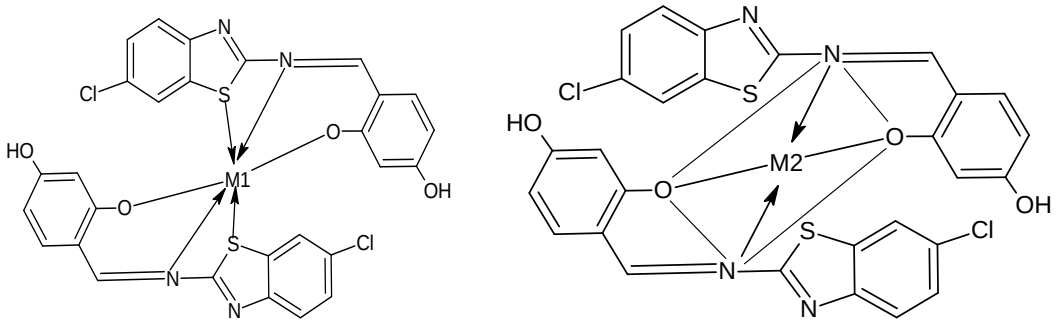

Where M1 = Mn(II), Fe(II), Co(II), Ni(II) and M2 = Cu(II), Pd(II), Zn(II), Cd(II), Hg(II)

References:

1. Wanninger, S., Lorenz, V., Subhan, A., & Edelmann, F. T. (2015). Metal complexes of curcumin–synthetic strategies, structures, and medicinal applications. *Chemical Society Reviews*, *44*(15), 4986-5002.
2. Hossain, M. S., Roy, P. K., Ali, R., Zakaria, C. M., & Kudrat-E-Zahan, M. (2017). Selected Pharmacological Applications of 1st Row Transition Metal Complexes: A review. *Clin. Med. Res*, *6*(6), 177-191.
3. Karges, J., Stokes, R. W., & Cohen, S. M. (2021). Metal complexes for therapeutic applications. *Trends in Chemistry*, *3*(7), 523-534.
4. Sodhi, R. K., & Paul, S. (2019). Metal complexes in medicine an overview and update from a drug design perspective. *Cancer Therapy & Oncology International Journal*, *14*(1), 25-32.
5. Khalaf, M. M., Abd El-Lateef, H. M., Gouda, M., Sayed, F. N., Mohamed, G. G., & Abu-Dief, A. M. (2022). Design, structural inspection, and bio-medicinal applications of some novel imine metal complexes based on acetylferrocene. *Materials*, *15*(14), 4842.
6. Malinowski, J., Zych, D., Jacewicz, D., Gawdzik, B., & Drzeżdżon, J. (2020). Application of coordination compounds with transition metal ions in the chemical industry review. *International Journal of Molecular Sciences*, *21*(15), 5443.
7. Wei, C., He, Y., Shi, X., & Song, Z. (2019). Terpyridine-metal complexes: Applications in catalysis and supramolecular chemistry. *Coordination chemistry reviews*, *385*, 1-19.
8. Takaya, J. (2021). Catalysis using transition metal complexes featuring main group metal and metalloid compounds as supporting ligands. *Chemical Science*, *12*(6), 1964-1981.
9. Larsen, C. R., & Grotjahn, D. B. (2017). The value and application of transition metal-catalyzed alkene isomerization in industry. *Applied Homogeneous Catalysis with Organometallic Compounds: A Comprehensive Handbook in Four Volumes*, 1365-1378.
10. Rafique, S., Idrees, M., Nasim, A., Akbar, H., & Athar, A. (2010). Transition metal complexes as potential therapeutic agents. *Biotechnology and Molecular Biology Reviews*, *5*(2), 38-45.
11. Karges, J., Stokes, R. W., & Cohen, S. M. (2021). Metal complexes for therapeutic applications. *Trends in Chemistry*, *3*(7), 523-534.
12. Hamzi, I. (2022). A Review of Biological Applications of Transition Metal Complexes Incorporating N-acylhydrazones. *Mini-Reviews in Organic Chemistry*, *19*(8), 968-990.
13. Nasiri Sovari, S., & Zobi, F. (2020). Recent studies on the antimicrobial activity of transition metal complexes of groups 6–12. *Chemistry*, *2*(2), 418-452.
14. Dar, O. A., Lone, S. A., Malik, M. A., Wani, M. Y., Ahmad, A., & Hashmi, A. A. (2019). New transition metal complexes with a pendent indole ring: insights into the antifungal activity and mode of action. *RSC advances*, *9*(27), 15151-15157.
15. Hassan, S. S., & Khalf-Alla, P. A. (2020). Anti-hepatocellular carcinoma, antioxidant, anti-inflammation, and antimicrobial investigation of some novel first and second transition metal complexes. *Applied Organometallic Chemistry*, *34*(4), e5432.
16. Liang, J. X., Zhong, H. J., Yang, G., Vellaisamy, K., Ma, D. L., & Leung, C. H. (2017). Recent development of transition metal complexes with in vivo antitumor activity. *Journal of Inorganic Biochemistry*, *177*, 276-286.

17. Shi, S., Yu, S., Quan, L., Mansoor, M., Chen, Z., Hu, H., ... & Liang, F. (2020). Synthesis and antitumor activities of transition metal complexes of a bis-Schiff base of 2-hydroxy-1-naphthalenecarboxaldehyde. *Journal of Inorganic Biochemistry*, *210*, 111173.
18. H.L. Singh, J. Singh, Bioinorg. Chem. Appl. 2014, 1 (2014)
19. J. Devi, S. Devi, A. Kumar, Heteroat. Chem. 27(6), 361 (2016)
20. A.A.R. Despaigne, G.L. Parrilha, J.B. Izidoro, P.R. da Costa, R.G. Santos, O.G. Piro, E.E. Castellano, W.R. Rocha, H. Beraldo, Eur. J. Med. Chem. 50, 163 (2012)
21. A. Kamal, M.A.H. Syed, S.M. Mohammed, Expert Opin. Ther. Pat. 25(3), 335 (2015)
22. S. Seth, Anti-Inflamm. Anti-Allergy Agents Med. Chem. 14(2), 98 (2015)
23. A.A. Weekes, A.D. Westwell, Curr. Med. Chem. 16(19), 2430 (2009).
24. Soni, P. L., & Soni, V. (2021). *The Chemistry of Coordination Complexes and Transition Metals*. CRC Press.
25. Sui, L. Z., Yang, W. W., Yao, C. J., Xie, H. Y., & Zhong, Y. W. (2012). Charge delocalization of 1, 4-benzenedicyclometalated ruthenium: a comparison between tris-bidentate and bis-tridentate complexes. *Inorganic Chemistry*, *51*(3), 1590-1598.
26. Kurdziel, K., & Głowiak, T. (2000). X-ray and spectroscopic characterization of octahedral cobalt (II) and nickel (II) complexes with 1-allyl imidazole in the solid state and electron-donor properties of the latter in aqueous solution. *Polyhedron*, *19*(20-21), 2183-2188.
27. Sato, T., & Nakamura, T. (1972). The complexes formed in the divalent transition metal-sulphuric acid-di-(2-ethylhexyl)-phosphoric acid extraction systems-cobalt (II), nickel (II), and copper (II) complexes. *Journal of Inorganic and Nuclear Chemistry*, *34*(12), 3721-3730.
28. Karipcin, F., Dede, B., Percin-Ozkorucuklu, S., & Kabalcilar, E. (2010). Mn (II), Co (II), and Ni (II) complexes of 4-(2-thiazolylazo) resorcinol: Syntheses, characterization, catalase-like activity, thermal and electrochemical behavior. *Dyes and Pigments*, *84*(1), 14-18.
29. Kalarani, R., Sankarganesh, M., Kumar, G. V., & Kalanithi, M. (2020). Synthesis, spectral, DFT calculation, sensor, antimicrobial, and DNA binding studies of Co (II), Cu (II), and Zn (II) metal complexes with 2-amino benzimidazole Schiff base. *Journal of Molecular Structure*, *1206*, 127725.
30. Spinu, C., & Kriza, A. (2000). Co (II), Ni (II) and Cu (II) complexes of bidentate Schiff bases. *Acta Chimica Slovenica*, *47*(2), 179-186.
31. Singh, P. K., & Kumar, D. N. (2006). Spectral studies on cobalt (II), nickel (II), and copper (II) complexes of naphthaldehyde substituted aroylhydrazones. *Spectrochimica Acta Part A: Molecular and Biomolecular Spectroscopy*, *64*(4), 853-858.
32. Kulkarni, A. D., Patil, S. A., & Badami, P. S. (2009). Electrochemical properties of some transition metal complexes: synthesis, characterization, and in-vitro antimicrobial studies of Co (II), Ni (II), Cu (II), Mn (II), and Fe (III) complexes. *International Journal of Electrochemical Science*, *4*(5), 717-729.
33. Yamabe, T., Hori, K., Minato, T., & Fukui, K. (1980). Theoretical study on the bonding nature of transition-metal complexes of molecular nitrogen. *Inorganic Chemistry*, *19*(7), 2154-2159.
34. Baiz, C. R., McRobbie, P. L., Anna, J. M., Geva, E., & Kubarych, K. J. (2009). Two-dimensional infrared spectroscopy of metal carbonyls. *Accounts of chemical research*, *42*(9), 1395-1404.
35. Falivene, L., & Cavallo, L. (2017). Theoretical NMR spectroscopy of N-heterocyclic carbenes and their metal complexes. *Coordination Chemistry Reviews*, *344*, 101-114.
36. Wenzel, T. J. (2013). Chiral derivatizing agents, macrocycles, metal complexes, and liquid crystals for enantiomer differentiation in NMR spectroscopy. *Differentiation of Enantiomers II*, 1-68.
37. Rahman, A. U. (2020). *Annual Reports on NMR Spectroscopy*. Academic Press.
38. Nandanwar, S. K., & Kim, H. J. (2019). Anticancer and antibacterial activity of transition metal complexes. *ChemistrySelect*, *4*(5), 1706-1721.
39. Mahmoud, N. F., Omar, N. R., Mohamed, G. G., & Sayed, F. N. (2022). Synthesis, structural characterization, and in vitro antibacterial activity studies of ternary metal complexes of anti-inflammatory bromhexine drug. *Inorganic Chemistry Communications*, 110216.
40. Bisceglie, F., Bacci, C., Vismarra, A., Barilli, E., Pioli, M., Orsoni, N., & Pelosi, G. (2020). Antibacterial activity of metal complexes based on cinnamaldehyde thiosemicarbazone analogs. *Journal of inorganic biochemistry*, *203*, 110888.
41. Rostamizadeh, S., Daneshfar, Z., & Moghimi, H. (2019). Synthesis of sulfamethoxazole and sulfabenzamide metal complexes; evaluation of their antibacterial activity. *European Journal of Medicinal Chemistry*, *171*, 364-371.
42. Chohan, Z. H., Mahmood-ul-Hassan, Khan, K. M., & Supuran, C. T. (2005). In-vitro antibacterial, antifungal, and cytotoxic properties of sulfonamide—derived Schiff's bases and their metal complexes. *Journal of Enzyme Inhibition and Medicinal Chemistry*, *20*(2), 183-188.